Thermochimica Acta, 203 (1992) 203–220
Elsevier Science Publishers B.V., Amsterdam

Thermoanalytical kinetics for solid state reactions as exemplified by the thermal dehydration of $Li_2SO_4 \cdot H_2O$

Haruhiko Tanaka [a], Nobuyoshi Koga [a] and Jaroslav Šesták [b]

[a] *Chemistry Laboratory, Faculty of School Education, Hiroshima University, Shinonome, Minami-Ku, Hiroshima 734 (Japan)*

[b] *Department of Chemistry, Institute of Physics, Czechoslovak Academy of Sciences, Na Slovance 2, CS-18040 Prague 8, (Czechoslovakia)*

(Received 25 June 1991)

Abstract

The fundamental problems in the thermoanalytical kinetics of solid state reactions were investigated as exemplified by the thermal dehydration of $Li_2SO_4 \cdot H_2O$. Distortion of the Arrhenius parameters and their consequent interdependence are described mathematically. A possible way to increase the reliability of the thermoanalytical kinetic study is discussed in connection with the possibility of the establishment of a kinetic standard.

INTRODUCTION

The thermoanalytical (TA) kinetic study of solid state reactions is a challenging task which aims at describing complicated heterogeneous processes by mathematical analysis at the phenomenological level for macroscopically averaged experimental data [1,2]. The kinetic procedure has been widely used with some success for both scientific and technological purposes. At the same time, a large number of philosophically oriented reviews on TA kinetics indicate that the method of kinetic study represents a limited approach [3–15]. The mis-estimation and/or over-estimation of the reliability of the TA kinetics have been causing incomplete understanding of the kinetics of solid state reactions.

The thermal dehydration of lithium sulfate monohydrate as a model reaction has been studied by several workers using TA methods [16–27]. Recent TA kinetic study on the reaction, complemented by microscopic observations, provided some more detailed information [22–24], but the problems inherent in the TA kinetic study were also pointed out [25,26]. In the present paper, the kinetics and mechanism of the thermal dehydration

Correspondence to: H. Tanaka, Chemistry Laboratory, Faculty of School Education, Hiroshima University, Shinonome, Minami-Ku, Hiroshima, 734, Japan.
Dedicated to Professor Joseph H. Flynn in honour of his 70th birthday.

of $Li_2SO_4 \cdot H_2O$ are reviewed in an attempt to scrutinize the fundamental problems in TA kinetics of solid state reactions. Distortion and/or interdependence of the kinetic parameters are treated as the most symbolic phenomena of these problems. The mechanism of the parameter interdependence is also reviewed from a mathematical point of view [28–30]. On the basis of the above consideration, the significance of the kinetic standard [31] and its possibility are briefly discussed.

It is hoped that these investigations provide a more fundamental understanding of our field of interest, i.e. the kinetics of solid state reactions, which in turn provides us with a valuable background for the further development and/or improvement of the kinetic procedure and thermoanalytical kinetics.

REACTION MORPHOLOGY

The thermal dehydration of lithium sulfate monohydrate is the reversible reaction expressed as

$$Li_2SO_4 \cdot H_2O \rightleftarrows Li_2SO_4 + H_2O \quad (1)$$

The reaction process of the dehydration consists of several chemical, physical and physicochemical events. One of the characteristics of the solid state reaction is the existence of reactive sites on the surface, i.e. crystal defects, linear dislocations, etc. When the reaction is accompanied by evolution of a gaseous product, as in eqn. (1), the reactivity is suppressed by the partial pressure of the gas within the matrix. Accordingly, the reaction starts from the surface, because of the higher diffusivity of the gaseous product.

Randomly distributed product particles of 0.2–1.0 μm, with rounded corners and sometimes equidimensional, were observed on the original surface of single crystals $Li_2SO_4 \cdot H_2O$ [23]. The area of the product particle assemblages spreads from each site of initial nucleation (Fig. 1). A significant feature in the growth of such assemblages is the development of subsurface pores or channels interconnecting neighboring nuclei. Surface reaction therefore proceeds by a nucleation and growth mechanism at the reaction interface. All the surface area is covered by these product crystallites at the fractional reaction, α, of less than 0.05. At the same time, the crack system, in which several cracks radiated from each central point, develops with the crack focuses at the initial nucleation sites. The distance between the neighboring focuses is 2–5 μm. The cracks may be produced by some volume contraction due to the dehydration and provide possible channels for the diffusion of water vapor produced at the reaction front advancing toward the center of the sample. The reaction behavior on the surface depends on the sample preparation. In the case of crushed crystals, the surface reaction takes place in the lower temperature region, which

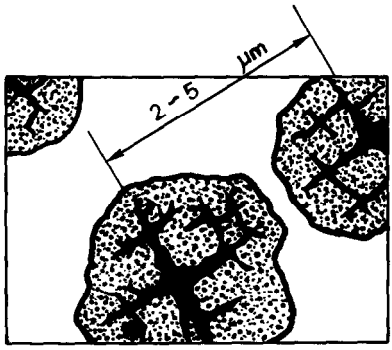

Fig. 1. Schematic representation of the surface reaction of the thermal dehydration of a single crystal of $Li_2SO_4 \cdot H_2O$.

may be due to mechanically roughened surface structure or the existence of amorphous phases.

Such a surface reaction leads to the rapid production of a solid product layer and a complete reactant–product interface advancing toward the center of the sample (Fig. 2) [22]. Product crystallites at the reaction interface are comparable in size with those on the surface, i.e. 0.2–1.0 μm. Thus the advancing reaction zone is composed on one side of the reactant and on the other of an irregular array of product crystallites. There is a positive tendency to develop fine channels extending significantly beyond the mean boundary, which is evidence of a zone of strain of appreciable thickness within the reactant [32,33]. As can be seen from the schematic representation in Fig. 2, a wavy front is formed on the reaction front proceeding along the *c* axis, whereas a flat front results on that advancing along the *a* axis. This difference in the reaction fronts seems to arise from changes in the nucleation density on the corresponding original surface and in the degree of stress and/or strain at the phase boundary, depending on the crystallographic direction. This may lead to different reactivity at the reaction interface and consequently to different reaction kinetics. Macro-

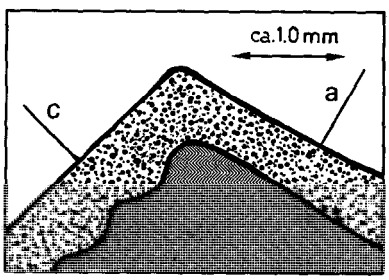

Fig. 2. Schematic representation of the internal (010) surface of a partially (approx. 40%) dehydrated single crystal of $Li_2SO_4 \cdot H_2O$.

scopically, the established reaction proceeds by the advancement of the reaction interface from the original surface to the center of the sample. The advancement is characterized by a nucleation and growth of the product crystallites, as is the case with the surface reaction, in which the overall process is controlled by bond rupture, diffusion of ions, nucleation, gaseous diffusion etc. Self-cooling at the reaction front and heat transfer are also important factors affecting the kinetics.

REACTION KINETICS BY THERMAL ANALYSIS

Single crystals

Table 1 summarizes the kinetic results reported for the isothermal dehydration of single crystals of $Li_2SO_4 \cdot H_2O$. Okhotnikov et al. [20] studied the kinetics for the propagation of the reaction interface towards a selected crystallographic direction, the [$\bar{1}$01] axis. The Arrhenius parameters obtained were correlated successfully with rupture of the Li–O bond accompanied by a 180° reorientation around the bisector of the HOH angle (flip motion). However, kinetic results from the other studies listed in Table 1 apparently represent information averaged over all the crystallographic directions in which the reaction interfaces advance [22,23]. Both of these studies showed that the overall behavior ($0.1 \leqslant \alpha \leqslant 0.9$) can be expressed satisfactorily either by the phase-boundary-reaction-controlled (R_n) law with $2 \leqslant n \leqslant 3$ or by the Avrami–Erofeev (A_m) law with $m \approx 2$. These kinetic obediences can be interpreted in relation to the reaction morphology, i.e. the reaction proceeds by advancing the reaction interface and the advancement itself depends on the nucleation and growth of the product crystallites, respectively. It was also shown that there are small but detectable variations in kinetics obedience with temperature and α. This was ascribed to variations, depending on the temperature and α, in the contribution from the reverse (rehydration) process and/or the relative rates of interface advance in different crystallographic directions. The kinetic parameters obtained under N_2 flow and in a vacuum are considerably different, showing kinetic compensation behavior (see below), although a comparable increasing trend in E as the reaction advances was observed for both sets of measurements. This conformity of kinetic characteristics in different ambient atmospheres is ascribed to the similar self-generated atmosphere inside the matrix of single crystals.

It was observed microscopically under polarizing light [22,24] that the reaction morphology or geometry under non-isothermal conditions was comparable with that observed isothermally. TA measurements under non-isothermal conditions at various heating rates, ϕ, were carried out using simultaneous TG–DSC [22,24], because the energy supplied from the DSC circuit decreases the distortion from linearity in the heating curve

TABLE 1

Kinetic results reported for the isothermal dehydration of single crystals of $Li_2SO_4 \cdot H_2O$

TA method	Atmosphere	Sample size	Temp. range (°C)	$g(\alpha)$ [a]	E (kJ mol^{-1})	log A (s^{-1})	Ref.
Quartz-crystal microbalance	Vacuum (4×10^{-5} Pa)	0.5 mm × 0.3 mm × 0.03 mm parallelepipeds	27–127	R_1 [$\bar{1}$01] axis	87.1 ± 0.8	14.2 ± 0.2	20
Simultaneous TG–DSC	N_2 flow (30 ml min^{-1})	15.0 mg	112–127	$R_{2.6}$ $A_{1.6}$	111.8 ± 3.2 111.8 ± 3.2	11.3 ± 0.4 11.7 ± 0.4	22
EGD (constant-volume glass apparatus)	Vacuum (1.5×10^{-2} Pa)	Approx. 20–40 mg	87–127	R_2 R_3 A_2	80.1 ± 3.4 79.9 ± 3.4 80.2 ± 3.4	6.9 ± 0.5 6.8 ± 0.5 7.2 ± 0.5	23

[a] Kinetic model function.

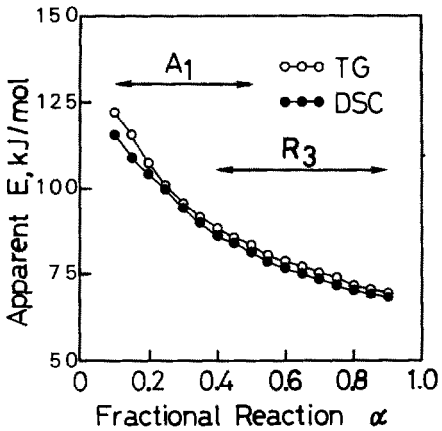

Fig. 3. Apparent values of activation energy calculated by the Ozawa method from simultaneous TG–DSC curves for the non-isothermal dehydration of single crystals of $Li_2SO_4 \cdot H_2O$ under N_2 flow ($1.0 \leqslant \phi$ K min$^{-1} \leqslant 8.0$).

caused by the enthalpy change during the reaction (see below). Figure 3 shows the activation energies E at various values of α from 0.1 to 0.9 in steps of 0.05. The E value decreases as the reaction advances, in contrast to the results observed for the isothermal process. The process was interpreted, on the whole, by a combination of an A_m law, which is representative of the earlier stage, and an R_n law, which becomes predominant as the reaction proceeds. The effect of the heating rate on the Arrhenius parameters is shown in Table 2. With increasing ϕ, the values of E and log A decrease, as is usually observed for the non-isothermal decomposition of solids. Physicochemically, the variations in the Arrhenius parameters have been explained by the tendency for the diffusion of water vapor through the solid product layer to become difficult with increasing α and ϕ [34]. In some cases, the process is actually controlled by the water vapor diffusion,

TABLE 2

The Arrhenius parameters calculated by the Coats and Redfern method for the non-isothermal dehydration of single crystals of $Li_2SO_4 \cdot H_2O$

ϕ (K min^{-1})	$0.1 \leqslant \alpha \leqslant 0.5$ ($A_1 = -\ln(1-\alpha)$)			$0.4 \leqslant \alpha \leqslant 0.9$ ($R_3 = 1-(1-\alpha)^{1/3}$)		
	E (kJ mol^{-1})	log A (s^{-1})	$-\gamma$ [a]	E (kJ mol^{-1})	log A (s^{-1})	$-\gamma$ [a]
0.47	272.0±4.2	33.2±0.6	0.9919	134.4±3.7	14.2±0.5	0.9950
0.95	251.8±4.0	30.4±0.5	0.9910	126.8±1.4	13.1±0.2	0.9999
1.89	196.5±2.3	22.5±0.3	0.9927	122.8±1.0	12.4±0.1	0.9967
4.02	153.5±1.5	16.8±0.2	0.9940	89.3±1.0	8.1±0.1	0.9989
8.04	117.7±1.2	12.1±0.2	0.9929	77.9±0.8	6.6±0.1	0.9976

[a] Correlation coefficient of the linear regression analysis of the Coats and Redfern plot.

TABLE 3

Kinetic results reported for the isothermal dehydration of crushed crystals of $Li_2SO_4 \cdot H_2O$

TA method	Atmosphere	Sample size	Temp. range (°C)	Range of α	$g(\alpha)$ [a]	E (kJ mol^{-1})	log A (s^{-1})	Ref.
TG–DSC	N_2 flow (30 ml min^{-1})	15.0 mg (−100+170 mesh)	85–99	0.1–0.9	$A_{2.4}$	90.2±0.5	9.7±0.1	22
				0.1–0.5	A_1	91.8±0.8	9.9±0.1	
				0.4–0.9	R_3	89.5±0.4	9.5±0.1	
EGD	Vacuum (1.5×10^{-2} Pa)	30.0 mg (−100+200 mesh)	76–104	0.1–0.9	D_4	91.6±1.8	9.2±0.3	23
				0.1–0.9	R_3	93.0±1.9	9.9±0.3	
				0.1–0.9	A_1	92.2±1.8	10.4±0.3	

[a] Kinetic model function.

especially during the later reaction stage at the higher heating rate. For such a process, some differences were observed between the kinetic results obtained from TG and DSC recorded simultaneously [35]. In the present reaction, however, no marked difference was observed as can be seen from Fig. 3. This seems to be because the escape routes for removal of the water vapor are established by the intercrystalline system of connected channels. Nevertheless, the partial pressure of water vapor at the reaction front presumably changes with α and ϕ. From this point of view, the partial pressure at the reaction interface cannot, in a strict sense, be specified in conventional TA measurements, even if the atmosphere outside the matrix is nominally controlled. Thus the different kinetic results arise not only from the change in the pre-determined measuring conditions, but also from the variation in the self-generated conditions during the reaction, which is also dependent on the measuring conditions.

Crushed crystals

Kinetic results reported for the isothermal dehydration of crushed crystals of $Li_2SO_4 \cdot H_2O$ are summarized in Table 3. Although a microscopic study of the dehydration process of crushed crystals ($-48 + 100$ mesh) [24] confirmed that the reaction under both isothermal and non-isothermal conditions proceeds by the advancement of the reaction interface from the original surface to the center of the particle, it was difficult to select the most appropriate kinetic model function from the TA measurements. This may be due to the fact that TA curves for the crushed crystals provide kinetic information averaged over all the different crystallographic directions and over all the particles in the sample matrix, in addition to the complexity of various physicochemical processes of the reaction. A kinetic analysis across the restricted ranges of α indicates that the earlier and later stages of the isothermal process can be satisfactorily described by the A_1 and R_3 laws respectively [22,24]. Comparable Arrhenius parameters were obtained under N_2 flow [22,24] and in a vacuum [23]. The activation energy, approx. 90 kJ mol^{-1}, corresponds superficially to the energy required to break all the relevant bonds, including the hydrogen bonds [20].

Table 4 lists the kinetic results obtained by the Ozawa method [36] from the TG (accompanied by DSC) curves at various values of ϕ in the range 0.5–8.0 K min^{-1}. The kinetic obedience across the restricted ranges of α shows a trend similar to that for the isothermal process, i.e. a combination of an A_m law and an R_n law, irrespective of the particle size fractions examined. Although the Arrhenius parameters obtained for the samples of $-48 + 100$ and $-100 + 170$ mesh are comparable, smaller values were observed for a $-170 + 200$ mesh sieve fraction. It is likely that this variation in the Arrhenius parameters can be ascribed to the fact that for the smaller particle size, both the surface area and defect density are larger

TABLE 4

Comparison of the kinetic parameters calculated by the Ozawa method from the TG curves accompanied by DSC for the non-isothermal dehydration of crushed crystals of various particle size fractions under N_2 flow ($0.5 \leqslant \phi$ K min$^{-1} \leqslant 8.0$)

Particle size (mesh)	Range of α	$g(\alpha)$ [a]	E (kJ mol^{-1})	log A (s^{-1})	γ [b]
−48+100	0.1–0.9	$R_{2.6}$	115.4±1.0	12.6±0.1	0.9999
	0.1–0.5	$A_{1.2}$	127.4±1.0	14.6±0.1	0.9999
	0.3–0.7	$R_{2.4}$	112.7±1.0	12.2±0.1	0.9999
	0.5–0.9	$R_{2.6}$	103.4±1.0	11.0±0.1	0.9999
−100+170	0.1–0.9	$R_{2.2}$	114.1±2.6	12.6±0.1	0.9999
	0.1–0.5	$A_{1.2}$	125.0±3.2	14.5±0.1	0.9999
	0.3–0.7	$R_{1.6}$	112.0±2.4	12.4±0.1	0.9999
	0.5–0.9	$R_{2.4}$	103.1±2.0	11.3±0.1	0.9998
−170+200	0.1–0.9	$R_{3.0}$	135.4±1.5	15.5±0.1	0.9999
	0.1–0.5	$A_{1.0}$	153.6±1.3	18.5±0.1	0.9998
	0.3–0.7	$R_{2.2}$	131.0±1.4	15.0±0.1	0.9999
	0.5–0.9	$R_{2.4}$	117.1±1.7	13.1±0.1	0.9998

[a] Kinetic model function.

[b] Correlation coefficient for the linear regression analysis of the $g(\alpha)$ vs. generalized time [22] plot.

and the particle radius is smaller. These changes enhance the reactivity of the surface, increase the rate of water vapor diffusion through the product layer in each particle and, in turn, decrease the rate of gross diffusion of water vapor through the assemblage of many particles, because of the narrower void space for the smaller particles.

In the case of the crushed crystals, the rate of gross diffusion of water vapor through the assemblage of particles is also retarded by larger sample sizes. Table 5 lists the effect of sample size on the kinetic results obtained for the isothermal dehydration of the crushed crystals (−100 + 170 mesh) [37]. Comparable results were observed for a sample of less than 20.0 mg. The Arrhenius parameters for a 25.0 mg sample are a little larger than

TABLE 5

Effect of the sample size on the kinetic parameters obtained for the isothermal dehydration of crushed crystals of $Li_2SO_4 \cdot H_2O$ (−100+170 mesh)

Sample size (mg)	$g(\alpha)$ [a]	E (kJ mol^{-1})	log A (s^{-1})	$-\gamma$ [b]
10.0	$A_{2.3}$	93.4±1.9	10.2±0.3	0.9901
15.2	$A_{2.4}$	90.2±0.5	9.7±0.1	0.9973
20.0	$A_{2.4}$	92.2±1.6	9.9±0.3	0.9912
25.1	$A_{2.7}$	103.3±2.5	11.4±0.4	0.9838

[a] Kinetic model function.

[b] Correlation coefficient for the linear regression analysis of the Arrhenius plot.

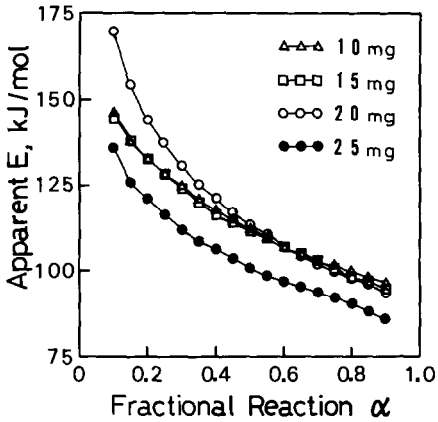

Fig. 4. Effect of the sample size on the activation energy calculated by the Ozawa method from the TG curves accompanied by DSC for the non-isothermal dehydration of crushed crystals of $Li_2SO_4 \cdot H_2O$ ($-100+170$ mesh) under N_2 flow ($0.5 \leqslant \phi$ K $min^{-1} \leqslant 8.0$).

those for a 20.0 mg sample, being accompanied by a slight but detectable change in the value of m in the A_m law. As shown in Fig. 4, a similar tendency was observed in non-isothermal processes for sample weighing 10.0–20.0 mg, although the E value decreases with increasing the sample size from 20.0 to 25.0 mg, in contrast to the isothermal process (Table 5). This may be ascribed to the comparable conditions of the self-generated gaseous atmosphere within the matrix between the samples of 10.0–20.0 mg. Although the simultaneous TG–DSC instrument was used to obtain the results shown in Table 5 and Fig. 4, the difference in the self-cooling effect due to the change in sample size may not be ignored. At the same time, the gaseous atmosphere affects directly the rate of gross diffusion of water vapor through the assemblage of sample particles [27].

Reliability of the TA kinetics

Although accurate determination of the sample temperature is essential in evaluating reliable kinetic parameters for solid state reactions, the measurement of temperature has always been and remains a serious problem [38,39]. In addition to the incorrect temperature measurement due to temperature gradients between the sample and temperature sensor, the programmed temperature conditions are distorted by self-cooling or self-heating effects, i.e. the enthalpy change during the reaction. Figure 5 shows typical curves of α against time, together with the heating curves, obtained by TG accompanied by power-compensation DSC and DTA at a programmed heating rate of 3.8 K min^{-1} for the non-isothermal dehydration of crushed crystals of $Li_2SO_4 \cdot H_2O$ [25]. The sample temperature on the TG–DSC system rises relatively more rapidly because of a reduction in the

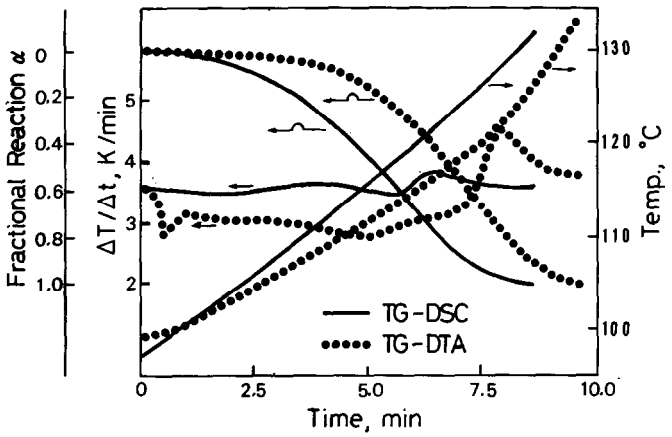

Fig. 5. Typical TG and temperatures curves, together with the $\Delta T/\Delta t$ vs. time plots, accompanied by DSC and DTA for the non-isothermal dehydration of crushed crystals of $Li_2SO_4 \cdot H_2O$ (−100+170 mesh) at a programmed heating rate of 3.8 K min^{-1} in N_2 flow.

self-cooling effect through the energy supplied from the DSC circuit. As expected for the TG–DTA system, the heating curve is far from linear during the reaction. The actual heating curve is more clearly illustrated by the plots of $\Delta T/\Delta t$ against t in Fig. 5, which are a measure of the fluctuation in heating rate from the linear heating of the sample. The curve for the TG–DSC run is smoother than that for TG–DTA, although the fluctuation increased with heating rate in both the TG–DSC and TG–DTA runs. Consequently, an apparent difference in the shape and/or slope between these two plots of α against t is observed, as shown in Fig. 5. Longer induction periods were observed for the TG curves accompanied by DTA. This may be ascribed to the longer time required for the sample to attain the reaction temperature, which is a result of endothermic water removal from the sample. Table 6 lists the kinetic parameters calculated by the Ozawa method from the TG curves accompanied by DSC and DTA at various ϕ values in the range 0.5–8.0 K min^{-1}. The reaction process is satisfactorily described by the R_3 law in the case of the TG–DTA measurements, in contrast to the α dependency of the kinetic obedience for the TG–DSC runs. One possible reason for this difference is likely to be the averaging of α over all the particles in the matrix during the induction periods in the TG–DTA runs. The variation in the Arrhenius parameters can be explained in connection with the change in the working temperature interval ΔT in the kinetic calculation (see below). The above kinetic difference is caused by the different temperature variations within the sample, because the experimental conditions are practically identical for the TG–DSC and TG–DTA experiments. In addition, any distortion from linearity in the increasing temperature also affects the kinetic parameters, because these are calculated by assuming a linear heating of the sample.

TABLE 6

Comparison of the kinetic parameters obtained by the Ozawa method from the TG curves accompanied by DSC and DTA for the non-isothermal dehydration of crushed crystals of $Li_2SO_4 \cdot H_2O$ (−100+170 mesh) in N_2 flow ($0.5 \leqslant \phi$ (K min^{-1}) $\leqslant 8.0$)

Range of α	TG–DSC				TG–DTA			
	$g(\alpha)$ [a]	E (kJ mol^{-1})	A (s^{-1})	γ [b]	$g(\alpha)$ [a]	E (kJ mol^{-1})	A (s^{-1})	γ [b]
0.1–0.9	$R_{2.2}$	114.1±2.5	4.0×10^{12}	0.9999	$R_{3.0}$	124.0±2.1	7.5×10^{13}	0.9987
0.1–0.5	$A_{1.2}$	125.0±3.2	1.2×10^{14}	0.9999	$R_{2.6}$	136.3±3.0	4.3×10^{15}	0.9999
0.2–0.6	$A_{1.3}$	117.7±2.7	1.3×10^{13}	0.9999	$R_{3.0}$	128.8±2.2	3.6×10^{14}	0.9997
0.3–0.7	$R_{1.6}$	112.0±2.4	2.6×10^{12}	0.9999	$R_{3.0}$	122.6±1.7	5.2×10^{13}	0.9998
0.4–0.8	$R_{2.3}$	107.3±2.2	4.8×10^{11}	0.9999	$R_{3.0}$	117.0±1.4	8.7×10^{12}	0.9998
0.5–0.9	$R_{2.3}$	103.1±2.0	1.3×10^{11}	0.9999	$R_{3.0}$	111.6±1.2	1.6×10^{12}	0.9995

[a] Kinetic model function.

[b] Correlation coefficient for the linear regression analysis of the $g(\alpha)$ vs. generalized time θ plot.

In using commercially available TA instruments with an active computer interface, it is sometimes difficult to detect the experimental problems related to the kinetics. It appears superficially that the TA curves obtained using such instruments are free from these problems. Figure 6 shows the activation energy calculated by isoconversion methods in terms of integral and differential equations, from computer-interfaced TG measurements for the isothermal dehydrations of crushed crystals of $Li_2SO_4 \cdot H_2O$ [26]. Different activation energies are obtained not only between the isothermal and non-isothermal measurements, but also between the integral and

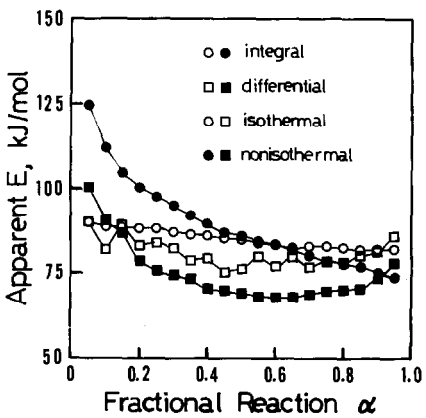

Fig. 6. Comparison of the apparent activation energies calculated by the integral and differential isoconversion methods from the conventional TG curves for the isothermal and non-isothermal dehydration of crushed crystals of $Li_2SO_4 \cdot H_2O$ (−100+170 mesh) in N_2 flow.

differential methods of kinetic evaluation. A similar trend is also observed for non-isothermal single-run methods. Although it is generally acceptable from the theoretical point of view that differential methods of kinetic calculation are more suitable in obtaining meaningful kinetic parameters than integral methods, it is evident that this depends on the reliability of the TA curves from the kinetic point of view. It must be remembered that TA techniques are based on measurements of the so-called thermal behavior, on detecting the reaction and/or transformations occurring, and on characterizing qualitatively the temperature region and rate. In this sense, the kinetic use of the TA curves is beyond their mean analytical capability, because kinetic study is based on the quantitative description of thermal behavior. The reliability is regulated by the degree of deviation in the actual reaction condition from that predetermined or idealized from the reaction itself, which depends on the kind of TA technique, the design of the equipment, the experimental conditions and the nature of the reaction under investigation.

Mutual interdependence of the Arrhenius parameters

In TA kinetic studies the apparent values of E and $\ln A$ change with sample preparation and measuring conditions, showing the mutual interdependence between these two Arrhenius parameters [40]. This is known as the kinetic compensation effect (KCE) and is expressed as

$$\ln A = \frac{1}{RT_{iso}} E + \ln k_{iso} \tag{2}$$

where R is the gas constant and T_{iso} is the so-called isokinetic temperature, at which rate constants of all the processes compared indicate the unique value, k_{iso}. The establishment of the KCE has been reported in many, diverse kinetic studies which have used TA methods, particularly where kinetic parameters for non-isothermal solid state reactions have been determined. Although much effort has been concentrated on the solution of this problem, it still remains a puzzle for many scientists [28,41–43]. In discussing the kinetic results of the present reaction, the KCE should be taken into account, as was stated above.

For the values of E and A, the following relationships can be derived, irrespective of the method of kinetic evaluation [30]:

$$E = \frac{RT_H T_L}{\Delta T} \ln X \tag{3}$$

$$\ln A = \frac{1}{T_{iso}} \frac{T_H T_L}{\Delta T} \ln X + \ln k_{iso} \tag{4}$$

where T_L and T_H are the lowest and highest temperatures of the kinetic analysis respectively, $\Delta T = T_H - T_L$ and X depends on the calculation method. The variation in the value of ln X due to the different reaction temperatures is relatively small compared with the change in the value of $T_H T_L/\Delta T$. This implies that a constant value of $T_H T_L/\Delta T$ is a necessary condition for obtaining a constant E value [5]. In this case, however, a constant value of ln A is not always obtained; the constant value of ΔT can yield constant Arrhenius parameters. This can be explained by the mathematical consequence of the above argument that for smaller values of ΔT, a slight change in $T_H T_L$ can be ignored in comparison with the change in $1/\Delta T$. When the KCE is established among several sets of Arrhenius parameters, the values of E and ln A are a function of $1/\Delta T$. It is clear that if the value of ΔT is small, a slight change in ΔT greatly affects the Arrhenius parameters and is one of the most important mathematical causations of the KCE. In the case of the TA measurements, the reaction temperature interval is sometimes restricted by the nature of the reaction under investigation and by the measuring condition applied, particularly under non-isothermal conditions. The change in the reaction and/or working temperature interval results from both experimental and physicochemical origins including the experimental error and self-generated reaction conditions, as exemplified by the thermal dehydration of $Li_2SO_4 \cdot H_2O$.

It was found that the KCE is also observed for the sets of Arrhenius parameters obtained from a single non-isothermal TA curve by the use of inappropriate kinetic model functions [33]. Somasekharan and Kalpagam reported recently [44] that in this type of KCE the T_{iso} corresponds closely to the peak temperature T_p of the TA curve. Taking into account the mathematical condition for the peak, the distortion of the Arrhenius parameters obtained using the inappropriate kinetic model function $h(\alpha)$ instead of the appropriate one $f(\alpha)$, can be expressed quantitatively by the following equations [29]:

$$\frac{E_{app}}{E} = \frac{f(\alpha_p)}{h(\alpha_p)} \frac{H(\alpha_p)}{F(\alpha_p)} \tag{5}$$

with $F(\alpha) = df(\alpha)/d\alpha$ and $H(\alpha) = dh(\alpha)/d\alpha$, and

$$\ln \frac{A_{app}}{A} = \frac{E}{RT_p} \left[\frac{f(\alpha_p)H(\alpha_p) - h(\alpha_p)F(\alpha_p)}{h(\alpha_p)F(\alpha_p)} \right] + \ln \frac{f(\alpha_p)}{h(\alpha_p)} \tag{6}$$

where E_{app} and A_{app} are the apparent Arrhenius parameters distorted by the use of $h(\alpha)$, and α_p is the fractional conversion at the peak. In the case of the KCE established by the use of various $h(\alpha)$, the slope of the compensation plot is a certain mean value determined by the relationship among the $f(\alpha)$ and $h(\alpha)$ examined. This explains the empirical fact that

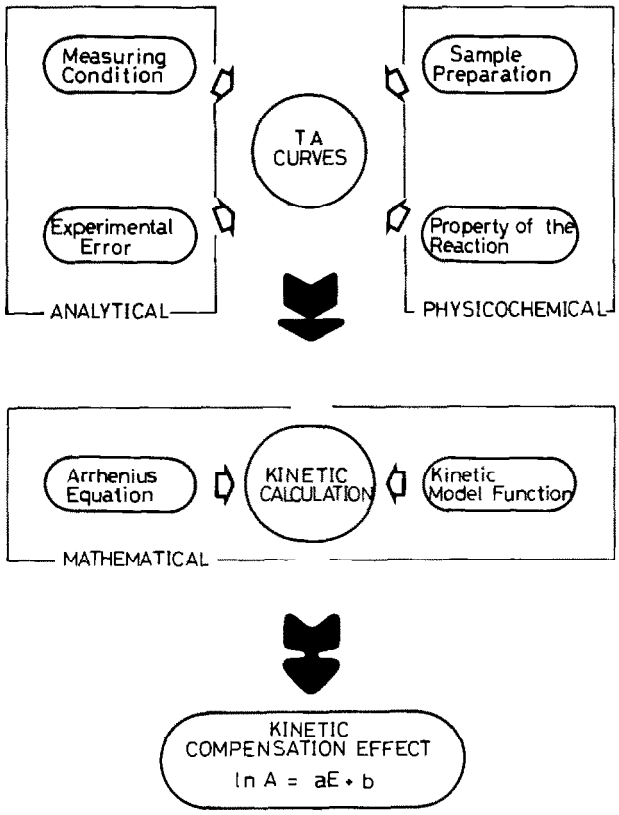

Fig. 7. Schematic representation of the procedure of the TA kinetics leading to the kinetic compensation effect.

the KCE of this type does not indicate a single intersecting point on the Arrhenius coordinate, i.e. an isokinetic point. The most important problem is whether or not the kinetics of solid state reactions is fully described by the rather oversimplified kinetic model function derived on the basis of physico-geometrical assumptions, besides the mis-estimation of the kinetic model function, because the actual process of the solid state reaction is more complicated, as illustrated by the reaction morphology of the thermal dehydration of $Li_2SO_4 \cdot H_2O$.

DISCUSSION

The major problems inherent in the practical study of TA kinetics are shown schematically in Fig. 7 [45]. Because the TA measurements give only the macroscopically averaged information about the process under investigation, changes in both the experimental and physicochemical factors influencing the kinetics of the process are detected as a change in the

position and shape of the TA curves. Such slight changes in the TA curves are projected to the KCE through the mathematical relationships described above. In this respect, the establishment of the KCE itself might not have any physical significance in formulating the kinetics of solid state reactions. On the contrary, it may suggest the unsuitability of such a kinetic approach.

The establishment of a "kinetic standard" seems to be a possible way of increasing the reliability of the TA kinetics [31]. According to Fig. 7, it is clear that some sort of standard is important in determining the reliability of the TA curves as a source of the kinetic data. At the same time, the kinetic standard should be based on the reaction with a selected sample under strictly restricted sample and measuring conditions, in which the kinetics are fully described by the present context. The characteristic points of the kinetic curve and/or the kinetic parameters determined using the most reliable TA technique are regarded as standard, and the reliability of a TA instrument for its kinetic use will be estimated by deviation from standard values. Such a kinetic standard should bring a universality to the kinetic results obtained from a TA measurement.

As described above, the reliability of the TA curves is determined, to some extent, by the degree of realization of the programmed or idealized reaction conditions. Concerning TA techniques, DSC or some TA techniques accompanied by DSC, are capable of following programmed temperature conditions. When the reaction is accompanied by the evolution of gas, constant rate thermal analysis [46] and/or quasi-isothermal quasi-isobaric thermal analysis [47] has the advantage that the self-generated gaseous atmosphere remains constant during the reaction, at least compared with conventional isothermal and non-isothermal TA methods. Even in this case, however, some interdependence of the kinetic parameters can be observed as a mathematical consequence [48]. It is desirable, in view of the measuring conditions, that reaction with small sample sizes proceeds at such a temperature where the speed of reaction is moderate. It must be noted that such a criterion regulates the working temperature interval and consequently leads to the establishment of the KCE. Some exothermic reactions, such as crystallization of glasses, satisfy the requirement of the kinetic standard [49] because excellent correspondence is sometimes observed among the Arrhenius parameters obtained thermoanalytically and from other physicochemical measurements [50]. Such a process has the characteristics that the temperature regions of nucleation and growth are relatively well separated and that the crystallization of the smaller and larger particles are regulated by the surface and bulk mechanism respectively [51]. Nevertheless, the selection of the ideal kinetic standard from the endothermic reactions which accompany evolution of gases, is extremely difficult owing to the applicability of the various TA techniques.

REFERENCES

1 J. Šesták, Thermophysical Properties of Solids, Elsevier, Amsterdam, 1984.
2 J. Šesták, J. Therm. Anal., 36 (1990) 1997.
3 J. Šesták, J. Therm. Anal., 16 (1979) 503; 33 (1988) 1263; Thermochim. Acta, 98 (1986) 339.
4 J. Blazejowski, Thermochim. Acta, 76 (1984) 359.
5 J.H. Flynn, J. Therm. Anal., 34 (1988) 365; 36 (1990) 1579.
6 M. Maciejewski, J. Therm. Anal., 33 (1988) 1269.
7 J.H. Flynn, M. Brown and J. Šesták, Thermochim. Acta, 110 (1987) 101.
8 J.H. Flynn, M. Brown, E. Segal and J. Šesták, Thermochim. Acta, 148 (1989) 45.
9 A.K. Galwey, Thermochim. Acta, 96 (1985) 259.
10 J. Zsakó, in Ž.D. Živković (Ed.), Thermal Analysis, Copper, Bor-Yugoslavia, 1984, p. 167.
11 T. Ozawa, Netsu, 1 (1974) 2.
12 K.N. Ninan, J. Therm. Anal., 35 (1989) 1267.
13 G. Pokol and G. Varhegyí, CRC Crit. Rev. Anal. Chem., 19 (1988) 65.
14 P.D. Garn, Thermochim. Acta, 135 (1988) 71; 169 (1990) 135.
15 J.M. Criado, J. Malek and J. Sestak, Thermochim. Acta, 175 (1991) 229.
16 G. Thomas and M. Soustelle, J. Chim. Phys. Phys.-Chim. Biol., 69 (1972) 1770.
17 V.G. Vasilev and Z.V. Ershova, Russ. J. Phys. Chem. (Engl. transl.), 46 (1972) 1197.
18 G. Bertrand, M. Lallemant and G. Watelle-Marion, J. Inorg. Nucl. Chem., 36 (1974) 1303.
19 H. Tanaka, Thermochim. Acta, 52 (1982) 195.
20 V.B. Okhotnikov, B.I. Yakobson and N.Z. Lyakhov, React. Kinet. Catal. Lett., 23 (1983) 125.
21 N.A. Kirdyashkina and V.B. Okhotnikov, React. Kinet. Catal. Lett., 36 (1988) 417.
22 N. Koga and H. Tanaka, J. Phys. Chem., 93 (1989) 7793.
23 A.K. Galwey, N. Koga and H. Tanaka, J. Chem. Soc., Faraday Trans., 86 (1990) 531.
24 N. Koga and H. Tanaka, Thermochim. Acta, 185 (1991) 135.
25 H. Tanaka and N. Koga, J. Therm. Anal., 36 (1990) 2601.
26 N. Koga and H. Tanaka, Abst. 2nd Japan–China Joint Symp. Calorimetry and TA, Osaka, 1990, p. 72; Thermochim. Acta, 183 (1991) 125.
27 J. Haung and P.K. Gallagher, in I.R. Harison (Ed.), Proc. 19th NATAS, Boston, 1990, p. 359, and personal communication, 1991.
28 N. Koga and J. Šesták, Thermochim. Acta, 182 (1991) 201.
29 N. Koga, J. Šesták and J. Malek, Thermochim. Acta, 188 (1991) 333.
30 N. Koga and J. Šesták, J. Therm. Anal., 37 (1991) 1103.
31 N. Koga and J. Šesták, Proc. 12th Czechoslovak Conf. on TA (Termanal '91), STU, Bratislava, 1991, p. 31.
32 V.V. Boldyrev, Y.A. Gaponov, N.Z. Lyakhov, A.A. Politov, B.P. Tolochko, T.P. Shkhtshneider and M.A. Sheromov, Nucl. Instr. Methods Phys. Res. Part A, 261 (1987) 192.
33 N. Koga and H. Tanaka, Solid State Ion., 44 (1990) 1.
34 P.K. Gallagher and D.W. Johnson, Jr., Thermochim. Acta, 6 (1973) 67.
35 H. Tanaka and N. Koga, Thermochim. Acta, 163 (1990) 295.
36 T. Ozawa, Bull. Chem. Soc. Jpn., 38 (1965) 1881.
37 N. Koga and H. Tanaka, in preparation.
38 J. Šesták, Talanta, 13 (1966) 567.
39 G. Varhegyí, Thermochim. Acta, 59 (1982) 31; 59 (1982) 43; 65 (1983) 333.
40 A.I. Lesnikovich and S.V. Levchik, J. Therm. Anal., 30 (1985) 237, 677.
41 R.K. Agrawal, J. Therm. Anal., 31 (1986) 73; 34 (1988) 1141; 35 (1989) 909.
42 J. Šesták, J. Therm. Anal., 32 (1987) 325.

43 J. Zsakó and N. Somasekharan, J. Therm. Anal., 32 (1987) 1277.
44 K.N. Somasekharan and V. Kalpagam, J. Therm. Anal., 32 (1987) 1471.
45 N. Koga, Ph.D. Thesis, Pardubice (ČSFR), 1991.
46 J. Rouquerol, J. Therm. Anal., 5 (1973) 203.
47 J. Paulik and F. Paulik, Anal. Chim. Acta, 56 (1971) 328.
48 D. Fatu and E. Segal, Thermochim. Acta, 61 (1983) 215.
49 J. Málek and V. Smrcka, Thermochim. Acta, 186 (1991) 153.
50 J. Šesták, in Z. Chvoj, J. Šesták and A. Triska (Eds.), Kinetic Phase Diagrams, Elsevier, Amsterdam, 1990, Chapter 6.
51 N. Koga, J. Šesták and Z. Strnad, Thermochim. Acta, 203 (1992) 361.